








## RESEARCH PAPER

# Identification of a critical binding site for local anaesthetics in the side pockets of K<sub>v</sub>1 channels

Aytug K. Kiper<sup>1</sup>  | Mauricio Bedoya<sup>2,3</sup>  | Sarah Stalke<sup>1</sup> | Stefanie Marzian<sup>1</sup> | David Ramírez<sup>4</sup>  | Alicia de la Cruz<sup>5,6</sup> | Diego A. Peraza<sup>5,6</sup>  | Alba Vera-Zambrano<sup>5,6,7</sup> | José C. E. Márquez Montesinos<sup>2</sup> | Bárbara A. Arévalo Ramos<sup>2</sup> | Susanne Rinné<sup>1</sup>  | Teresa Gonzalez<sup>5,6,7</sup> | Carmen Valenzuela<sup>5,6</sup>  | Wendy Gonzalez<sup>2,3</sup> | Niels Decher<sup>1</sup> 

<sup>1</sup>Institute for Physiology and Pathophysiology, Philipps-University Marburg, Marburg, Germany

<sup>2</sup>Centro de Bioinformática y Simulación Molecular, Universidad de Talca, Talca, Chile

<sup>3</sup>Millennium Nucleus of Ion Channels-Associated Diseases (MiNICAD), Universidad de Talca, Talca, Chile

<sup>4</sup>Instituto de Ciencias Biomédicas, Universidad Autónoma de Chile, Santiago, Chile

<sup>5</sup>Instituto de Investigaciones Biomédicas Alberto Sols, Consejo Superior de Investigaciones Científicas (CSIC) and Universidad Autónoma de Madrid (UAM), Madrid, Spain

<sup>6</sup>Spanish Network for Biomedical Research in Cardiovascular Research (CIBERCV), Instituto de Salud Carlos III, Madrid, Spain

<sup>7</sup>Biochemistry Department, School of Medicine, Universidad Autónoma de Madrid, Madrid, Spain

## Correspondence

Carmen Valenzuela, Instituto de Investigaciones Biomédicas Alberto Sols, Consejo Superior de Investigaciones Científicas (CSIC) and Universidad Autónoma de Madrid (UAM), Madrid, Spain.  
Email: cvalenzuela@iib.uam.es

Wendy Gonzalez, Centro de Bioinformática y Simulación Molecular, Universidad de Talca, Talca, Chile.  
Email: wgonzalez@utalca.cl

Prof. Dr Niels Decher, Institute for Physiology and Pathophysiology, Philipps-University Marburg, Deutschhausstraße 2, 35037 Marburg, Germany.  
Email: decher@staff.uni-marburg.de

## Funding information

Consejo Superior de Investigaciones Científicas, Grant/Award Numbers: 2019AEP148, PIE201820E104; Deutsche

**Background and Purpose:** Local anaesthetics block sodium and a variety of potassium channels. Although previous studies identified a residue in the pore signature sequence together with three residues in the S6 segment as a putative binding site, the precise molecular basis of inhibition of K<sub>v</sub> channels by local anaesthetics remained unknown. Crystal structures of K<sub>v</sub> channels predict that some of these residues point away from the central cavity and face into a drug binding site called side pockets. Thus, the question arises whether the binding site of local anaesthetics is exclusively located in the central cavity or also involves the side pockets.

**Experimental Approach:** A systematic functional alanine mutagenesis approach, scanning 58 mutants, together with in silico docking experiments and molecular dynamics simulations was utilized to elucidate the binding site of bupivacaine and ropivacaine.

**Key Results:** Inhibition of K<sub>v</sub>1.5 channels by local anaesthetics requires binding to the central cavity and the side pockets, and the latter requires interactions with residues of the S5 and the back of the S6 segments. Mutations in the side pockets

**Abbreviations:** A/D, analogue/digital; I/V, current-voltage relationship; I<sub>control</sub>, current in the absence of drug; I<sub>drug</sub>, current in the presence of drug; I<sub>Kur</sub>, ultrarapid delayed rectifier current; MD, molecular dynamics; MM/GBSA, molecular mechanics with generalized Born and surface area continuum solvation; PDB, Protein Data Bank; POPC, 1-palmitoyl-2-oleoyl-sn-glycero-3-phosphocholine; RMSD, root-mean-square deviation; SASA, solvent-accessible surface area; SPC, single point charge; V<sub>1/2</sub>, voltage at half-maximal activation; ΔΔE<sub>c</sub>, coupling energy; θ, degree of stereoselectivity.

Aytug K. Kiper, Mauricio Bedoya, Sarah Stalke and Stefanie Marzian are joint first authors.

This is an open access article under the terms of the Creative Commons Attribution License, which permits use, distribution and reproduction in any medium, provided the original work is properly cited.

© 2021 The Authors. *British Journal of Pharmacology* published by John Wiley & Sons Ltd on behalf of British Pharmacological Society.

Forschungsgemeinschaft, Grant/Award Number: DE1482/4-1; Fondecup, Grant/Award Number: 160063; Fondo Europeo de Desarrollo Regional (FEDER), Grant/Award Number: CB/11/00222; Fondo Nacional de Desarrollo Científico y Tecnológico, Grant/Award Number: 1191133; Ministerio de Ciencia e Innovación, Grant/Award Number: SAF2016-75021-R and PID2019-104366RB-C21

remove stereoselectivity of inhibition of  $K_v1.5$  channels by bupivacaine. Although binding to the side pockets is conserved for different local anaesthetics, the binding mode in the central cavity and the side pockets shows considerable variations.

**Conclusion and Implications:** Local anaesthetics bind to the central cavity and the side pockets, which provide a crucial key to the molecular understanding of their  $K_v$  channel affinity and stereoselectivity, as well as their spectrum of side effects.

#### KEYWORDS

bupivacaine,  $K_v1$  channels, local anaesthetics, ropivacaine, side pockets, stereoselectivity

## 1 | INTRODUCTION

Local anaesthetics block sodium channels by binding to their open and/or inactivated state, along with stabilizing their slow inactivation (Bennett et al., 1995; Valenzuela, Snyders, et al., 1995). These sodium channel modulations provide the molecular basis for the block of pain perception. However, local anaesthetics also block a variety of cardiac ion channels, which partly contributes to the cardiotoxicity of local anaesthetics (Clarkson & Hondeghem, 1985; Lipka et al., 1998; Valenzuela, Delpon, et al., 1995). **Bupivacaine** for instance is a long-acting local anaesthetic, which increases heart rate and arterial BP, reduces cardiac stroke volume and ejection fraction, decreases conductivity and contractility and tends to induce arrhythmias and a long QT syndrome (Clarkson & Hondeghem, 1985; Kotelko et al., 1984; Sanchez-Chapula, 1988; Scott et al., 1989).

**$K_v1.5$  channels** that generate the ultrarapid delayed rectifier current  $I_{Kur}$  regulate atrial action potential durations (Fedida et al., 1993; Snyders et al., 1993) and are major drug targets for the treatment of atrial fibrillation (Decher et al., 2006; Kiper et al., 2015).  $K_v1.5$  channels are blocked by bupivacaine in a potent and stereoselective manner (Franqueza et al., 1997; Valenzuela, Delpon, et al., 1995). Voltage-gated ion channels share the common feature of a water filled central cavity containing the classical drug binding site in the inner mouth of the channel. The binding sites are mostly formed by two to three amino acid residues of the pore-forming helices and one to two residues located in the pore helix. The position of the residues involved in drug binding within these regions is highly conserved from sodium over calcium to different potassium channels (Decher et al., 2004, 2006; Hanner et al., 2001; Hockerman et al., 2000; Mitcheson et al., 2000). The recently identified side pockets in voltage-gated potassium ( $K_v$ ) channels formed by the back of the S5 and S6 segments together with the S4 and the S4–S5 linker of the neighbouring subunit serve as a drug binding pocket, providing the molecular basis for an allosteric and irreversible  $K_v1.x$ -specific channel inhibition (Marzian et al., 2013).

In early seminal studies probing the pore of  $K_v$  channels, it was reported that mutations affecting T441 and T469 of the *Drosophila*  $K_v1$ -related *Shaker* channel alter open-channel block of quaternary ammonium compounds (Choi et al., 1993; Yellen et al., 1991). Thus, open-channel block was proposed to require, as described above for

### What is already known

- $K_v1.5$  channels are blocked by local anaesthetics in a potent and stereoselective manner.
- Side pockets provide drug binding sites for  $K_v1.x$  channel blockers.

### What does this study add

- Local anaesthetics bind to the central cavity and the side pockets of  $K_v1.5$  channels.
- Binding to side pockets of  $K_v1.5$  channels determines efficiency and stereoselectivity of local anaesthetic inhibition.

### What is the clinical significance

- Side pockets provide the molecular basis to modulate the efficiency and side effects of antiarrhythmics.

many channels in detail, binding to two sites, one located in the pore loop and one located in the inner mouth of the channel (Baukrowitz & Yellen, 1996). The two residues identified in these early studies correspond, in  $K_v1.5$  channels to residues T479 in the pore signature sequence and T507 of the S6 segment. Furthermore, L510 was discussed as an important drug binding residue in  $K_v1.5$  channels, as studies with the homologous  $K_v2.1$  and  $K_v3.1$  channels showed an altered pharmacology for mutants corresponding to L510 (Aiyar et al., 1994; Shieh & Kirsch, 1994). These observations, together with a helical wheel blot analyses led to the misinterpretation that T479, T507, L510 and V514 line the inner cavity of the  $K_v1.5$  channel pore, forming the drug binding site of the channel (Yeola et al., 1996). Subsequent studies investigated the role of these putatively pore-facing residues as possible binding sites for local anaesthetics like bupivacaine (Franqueza et al., 1997) and benzocaine (Caballero et al., 2002), but also **rupatadine** (Caballero et al., 1999) and **irbesartan** (Moreno et al., 2003). The crystal structure of the closely

related  $rK_v1.2$  channels (Long et al., 2005) revealed however that the amino acids T507, L510 and V514 are not pore facing. In contrast, T507 and L510 perfectly face into the recently identified side pockets that play a crucial role for the development of  $K_v1.x$  channel-specific blockers (Marzian et al., 2013). This led to the question whether bupivacaine and other local anaesthetics exclusively interact with the central cavity or also require interactions with the newly identified side pockets (Marzian et al., 2013).

To address this question, we mapped the binding site of the two local anaesthetics bupivacaine and ropivacaine using a systematic functional alanine scanning mutagenesis screen of the S4, S4–S5, S5 and the S6 segments of  $K_v1.5$ , combined with in silico docking experiments and molecular dynamics (MD) simulations. Our results reveal that local anaesthetics do not exclusively bind to the central cavity and that binding to the side pockets is critical for the action of local anaesthetics. In addition, we found that a binding of local anaesthetics to the central cavity and the side pockets is conserved, whereas the binding modes show considerable variations, which might provide the molecular basis to modulate specificity and stereoselectivity, and thus the side effects of local anaesthetics.

## 2 | METHODS

### 2.1 | Molecular biology

PCR-based mutagenesis was used to insert mutations into the h $K_v1.5$  ( $KCNA5$ ) cDNA. The  $K_v1.5$  channel cDNA is based on the database entry NM\_002234 but differs by two residues (K418R and K565E). Compared with the previous database entry M60451, it includes two additional amino acids in the N-terminus, leading to a shift of the numbering of +2. The PCR products were fully sequenced (ABI 3100, Applied Biosystems, California, USA).  $K_v1.5$  cDNA was linearized with *NheI*, and complementary cRNA was produced with the mMACHINE T7-Kit (AM1344–Ambion, Texas, USA), and its quality was checked by UV spectroscopy (NanoDrop 2000–Thermo Fisher Scientific, Texas, USA, RRID:SCR\_020309) and gel electrophoresis.

### 2.2 | Injection and voltage-clamp recordings in *Xenopus* oocytes

All animal care and experimental procedures conformed to the Guide for the Care and Use of Laboratory Animals (NIH Publication 85-23), and the local ethics commission of the ‘Regierungspräsidium Giessen’ approved the experiments using *Xenopus* frogs (Nasco, Wisconsin, USA) (MR 20/28 Nr. A 23/2017). Animal studies are reported in compliance with the ARRIVE guidelines (Percie du Sert et al., 2020) and with the recommendations made by the *British Journal of Pharmacology* (Lilley et al., 2020). As we utilized *Xenopus laevis* oocytes as a heterologous expression system in this study, and the isolation of oocytes is by nature only possible from female frogs, we are using a unisex experimental background. Nevertheless, the resulting data are

transferrable to both sexes, considering that the function of the expressed ion channels and their direct pharmacological modulation are not sex specific. *X. laevis* oocytes provide a well-established heterologous expression system in the field of ion channel research without any reports of sex-specific effects. Thus, our conclusions are most likely to be valid in the context of male-derived experimental systems.

The cRNA for wild-type or mutant  $K_v1.5$  constructs was injected into isolated stage IV and V *X. laevis* oocytes as described previously (Streit et al., 2011). The oocytes were cultured in bath solution including (in mM): 96 NaCl, 2 KCl, 1  $MgCl_2$ , 1.8  $CaCl_2$  and 5 HEPES, pH 7.5, supplemented with 50-mg·L<sup>-1</sup> gentamycin, 274-mg·L<sup>-1</sup> sodium pyruvate and 88-mg·L<sup>-1</sup> theophylline at 18°C for 1–13 days before the experiments. All measurements were performed using standard two microelectrode voltage-clamp techniques (Stühmer, 1992). Measurements were recorded at room temperature (21–23°C) with a TurboTEC 10 CD amplifier (npi electronic, Tamm, Germany) and a Digidata 1200 Series analogue/digital (A/D) converter (Molecular Devices, California, USA). Micropipettes with a resistance of 0.5–1.2 M $\Omega$  when filled with 3 mM KCl were made from borosilicate glass capillaries GB 150TF-8P (Science Products, Hofheim, Germany) and pulled with a DMZ-Universal Puller (Zeitz, Martinsried, Germany, RRID:SCR\_014774). *R/S*-bupivacaine and ropivacaine were prepared as a 125 mM stock solution in DMSO, stored in lightproof containers and added to the bath solution just before the recordings. The holding potential was –80 mV. To guarantee a full regeneration from inactivation, a minimum interpulse interval of 10 s was chosen. The inhibition was calculated at the end of a voltage step to +40 mV for 2 s. An endogenous current component of the oocytes in amount of 150 nA has been subtracted in the analysis to increase the sensitivity of the scan. The ratio  $I_{drug}/I_{ctrl}$  was also determined using this protocol. The current corresponding to the first pulse after a 12-min pulse-free period in the presence of drug was divided by the last trace in the absence of drug before the pulse-free period. The *I/V* protocol, which was used to obtain the current–voltage relationship (*I/V*), comprises 10-mV steps in voltage, ranging from –70 to +70 mV for 200 ms, and a final step to –40 mV for 300 ms. A Hill plot was used to calculate the half-maximal inhibitory concentration ( $IC_{50}$ ). Boltzmann plot was used to calculate the voltage at half-maximal activation ( $V_{1/2}$ ).

### 2.3 | Patch-clamp recordings with bupivacaine enantiomers and side pocket mutants

HEK-293 cells were transfected with  $K_v1.5$  cloned in pcDNA3.1 as previously described (Arias et al., 2007; Gonzalez et al., 2002). The intracellular pipette filling solution contained (mM): K aspartate 80, KCl 42, phosphocreatine 3,  $KH_2PO_4$  10, MgATP 3, HEPES-K 5 and EGTA-K 5, and was adjusted to pH 7.25 with KOH. The bath solution contained (mM): NaCl 145, KCl 4,  $CaCl_2$  1.8,  $MgCl_2$  1.0, HEPES Na 10 and glucose 10, and was adjusted to pH 7.40 with NaOH. Both bupivacaine enantiomers were dissolved as stock solutions in deionized MilliQ water at a concentration of 100 mM.  $K_v1.5$  channel currents were recorded at room temperature (21–23°C) using

the whole-cell patch-clamp technique (Hamill et al., 1981) with an Axopatch 200B patch-clamp amplifier and a Digidata 1440A A/D converter (Molecular Devices, California, USA). Currents were filtered at 2 kHz (four-pole Bessel filter) and sampled at 4 kHz. Micropipettes were pulled from borosilicate glass capillary tubes (Narishige, GD-1, Tokyo, Japan) on a programmable horizontal puller (Sutter Instruments Co., California, USA) and heat polished with a microforge (Narishige, Japan). Micropipette resistance was 2–4 M $\Omega$ . Capacitance and series resistance compensation were optimized, and 80% compensation of effective access resistance was usually obtained. Cells were held at –80 mV, and 250-ms pulses between –80 and +60 mV (in 10-mV steps) were applied at a frequency of 0.1 Hz in order to avoid accumulation of inactivation. Deactivating tail currents were recorded at –40 mV. The IC<sub>50</sub> and Hill coefficients,  $n_H$ , were obtained from fitting the fractional block at various S- or R-bupivacaine concentrations to a Hill plot. The degree of stereoselectivity ' $\theta$ ' was calculated as fold difference of half-maximal inhibitory concentrations between S-bupivacaine and R-bupivacaine. Coupling energies ' $\Delta\Delta E_\Omega$ ' were calculated via mutant cycle analyses as previously described (Hidalgo & MacKinnon, 1995) (Figure S1). Error propagation has been used to calculate the SD of ' $\theta$ ' and ' $\Delta\Delta E_\Omega$ ' values, as they were originally acquired from a single IC<sub>50</sub> value with an SD.

## 2.4 | Homology modelling of the K<sub>v</sub>1.5 channel

The K<sub>v</sub>1.5 channel model previously reported by our group was used to study the binding site for local anaesthetics (Marzian et al., 2013). Briefly, the crystal structure of the open-state K<sub>v</sub>1.2–K<sub>v</sub>2.1 chimera (Protein Data Bank [PDB] code: 2R9R) (Long et al., 2007) was used as template. The modelled transmembrane region of K<sub>v</sub>1.5 includes the residues 269–526, which correspond to residues 160–417 of the template. Modeller 9v5 (Sali & Blundell, 1993) was used to create the K<sub>v</sub>1.5 homology model.

## 2.5 | Docking of bupivacaine and ropivacaine

In order to study the binding site and mode of local anaesthetics in the K<sub>v</sub>1.5 ion channel, we used a systematic pipeline that included docking simulations in the central cavity and in one side pocket followed by MD simulations and clustering of conformers. Briefly, two binding sites were selected in the K<sub>v</sub>1.5 homology model, the central cavity and one side pocket. We carried out the docking of local anaesthetics into only one side pocket because the other three are integrated by the same residues due to the tetrameric nature of the functional channel. Ligands were prepared using LigPrep module (LigPrep, Schrödinger, LLC, New York, NY, 2017-1). Energy minimization in the gas phase using MacroModel (MacroModel, Schrödinger, LLC, New York, NY, 2017-1, RRID:SCR\_016747) with the OPLS2005 force field was performed. The ligand parameters and charges were added according to the OPLS2005 force field (Banks et al., 2005; Kaminski et al., 2001; Shivakumar et al., 2010). The nitrogen atom of the piperidine ring was

protonated for both ligands. The charges were maintained during the parametrization process before docking and MDs. The docking simulations were performed with Glide (Friesner et al., 2006) using the standard precision scoring function, obtaining 10 poses per docking simulation. The centre of the grid boxes for each binding site was focused using the interacting residues identified by the functional alanine mutagenesis approach for each local anaesthetic (Figure S2). All molecular docking runs were performed with the outer box edge of the grid setting as 30 Å, thus ensuring that the binding site residues were included in each grid box. A rescoring of the energy was performed calculating the binding free energy using the molecular mechanics with generalized Born and surface area continuum solvation (MM/GBSA) method (Guimaraes & Cardozo, 2008; Ramirez et al., 2017). Then the pose selected per docking simulation was taken from those with the lowest MM/GBSA energy. The best poses according to the docking score were further studied by MD simulations.

## 2.6 | MD simulations

The selected poses in the side pocket were triplicated in the other side pockets. The selected pose in the central cavity was also included forming a complex with five ligands, four in each side pocket and one in the central cavity. The protein–ligand complexes were embedded into a pre-equilibrated 1-palmitoyl-2-oleoyl-*sn*-glycero-3-phosphocholine (POPC) bilayer, and then the systems were solvated using the single point charge (SPC) water model. K<sup>+</sup> ions were placed at Sites S2 and S4 of the selectivity filter and water molecules at Sites S1 and S3. Cl<sup>–</sup> ions were added to neutralize the system. An ion concentration of 0.15-M KCl on both sides of the channel was set for the MDs. The systems were equilibrated by 20 ns in NPT ensemble with positional restraints of 1.0 kcal·mol<sup>–1</sup>·Å<sup>–2</sup> on the secondary structure of the protein, ligands and ions at the selectivity filter. Temperature and pressure were kept constant at 300 K and 1.01325 bar, respectively, by coupling to a Nosé–Hoover chain thermostat (Cheng & Merz, 1996) and Martyna–Tobias–Klein barostat (Martyna et al., 1994) with an integration time step of 2 fs. Later, positional restraints were removed, and an MD simulation of 100 ns was done per system using an NP $\gamma$ T (semi-isotropic ensemble) with constant surface tension of 0.0 bar Å as production. MD simulations were performed using Desmond (Bowers et al., 2006) software, v2019-1 and OPLS2005 force field (Banks et al., 2005; Shivakumar et al., 2010). The same MD protocol was applied to the K<sub>v</sub>1.5 protein (without ligands) as control. From the 100-ns MDs of production, 200 structures from the last 20 ns (every 0.1 ns) were selected to perform the clustering analysis of both ligands (S-bupivacaine and ropivacaine) in each binding site. Protein structure of the selected frames was aligned, and then the cluster analysis was performed by selecting the heavy atoms of the ligand with a defined root-mean-square deviation (RMSD) cut off = 2 Å. Clusters were calculated using the Clustering v2.0.1 plugin (Github June 2014) in the VMD software (University of Illinois, Illinois, USA). To perform the analysis of the contact surface area, the PyMOL software (The PyMOL Molecular Graphics System, Version 2.0, Schrödinger, LLC, RRID:SCR\_000305)



and the 'Contact surface analyzer' script were used, using the solvent-accessible surface area (SASA) overlapped between the ligands and the protein. For the hydrogen bond analysis, the VMD software (Humphrey et al., 1996) and the script 'hbonds' from the VMDTools repository were used. The balance descriptors of the binding site of each ligand in the last 20 ns of each simulation were calculated with SiteMap module of the Schrödinger suite (SiteMap, Schrödinger, LLC, New York, NY, 2019) (Halgren, 2007, 2009). The data correspond to 84 values for each system (four ligands per frame, 21 frames from the last 20 ns of MD simulations). Each site was defined considering the coordinates of the pose of each ligand in each frame, with a 'sitebox' parameter of 5 Å. The balance descriptor corresponds to a ratio between the hydrophobic (phobic) and the hydrophilic (philic) scores of the site. Therefore, the higher the values for the balance descriptor, the more hydrophobic is the binding site.

## 2.7 | Data and statistical analysis

The data and statistical analysis comply with the recommendations of the *British Journal of Pharmacology* on experimental design and analysis in pharmacology (Curtis et al., 2018). We did not utilize statistical methods to predetermine sample or group sizes, and the numbers of necessary experiments were estimated on the basis of previous experiments/literature in the field. In addition, no exclusion criteria were pre-established, and no data were excluded from the subsequent analysis. For the experiments, no randomization or blinding was performed. Currents carried by wild-type  $K_v1.5$  channels directly before drug application were used for normalization for each individual oocyte in order to minimize variation. Normality of the data set was tested with a Shapiro–Wilk test, and subsequently, equality of variance was tested using either parametric or non-parametric Levene's test. An unpaired Student's *t* test was used to probe the significance, but for non-normally distributed data, the Mann–Whitney *U*-test. If the variances of the data set were significantly different, statistical significance of the data set was probed with Welch's *t* test and for non-normally distributed data with Mood's median test. All data are presented as mean  $\pm$  SEM (except Figure 2e,f). The number of biological replicates (*n*) is illustrated in the respective figure legends or graphs. The declared group size is the number of these biological replicates, and the statistical analysis was performed using these independent values. Values of  $P < .05$  were taken to show significant differences between group means in the figures. Data were acquired with pClamp 10 (Molecular Devices, California, USA, RRID:011323) and analysed with Clampfit (Molecular Devices, California, USA, RRID:011323), Excel 2016 (Microsoft, Washington, USA) and OriginPro 2018 (OriginLab, Massachusetts, USA, RRID:SCR\_002815).

## 2.8 | Materials

Gentamicin, sodium pyruvate, theophylline, *R/S*-bupivacaine and ropivacaine were purchased from Sigma-Aldrich (Missouri, USA).

*R*-bupivacaine and *S*-bupivacaine enantiomers were obtained from AstraZeneca® (London, UK) directly.

## 2.9 | Nomenclature of targets and ligands

Key protein targets and ligands in this article are hyperlinked to corresponding entries in <http://www.guidetopharmacology.org> and are permanently archived in the Concise Guide to PHARMACOLOGY 2019/20 (Alexander et al., 2019).

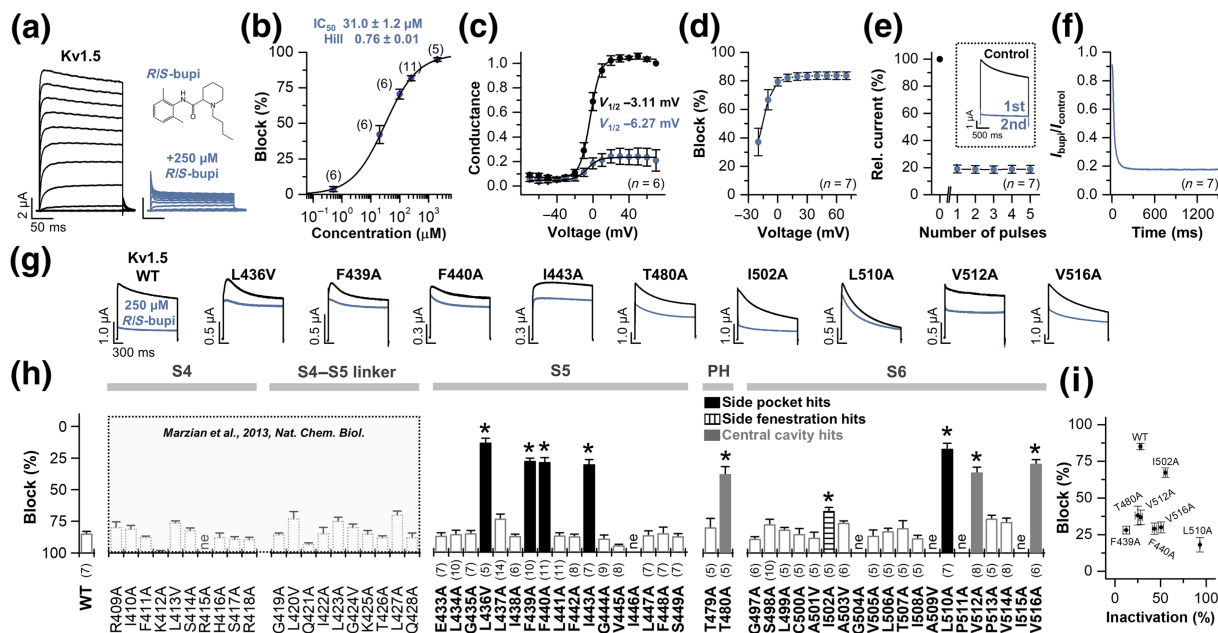
## 3 | RESULTS

### 3.1 | Analysis of $K_v1.5$ channel inhibition by bupivacaine

First, we analysed the inhibition of  $K_v1.5$  channels by racemic *R/S*-bupivacaine using the *X. laevis* oocyte expression system (Figure 1a). The  $IC_{50}$  of bupivacaine was  $31.0 \pm 1.2 \mu\text{M}$  with a Hill coefficient of  $0.76 \pm 0.01$  (Figure 1b and Table S1). Bupivacaine did not cause a major shift in the voltage dependence of the activation curve of  $K_v1.5$  channels (Figure 1c). The inhibition of  $K_v1.5$  channels by bupivacaine was reversible (Figure S3) and voltage dependent, as previously described (Gonzalez et al., 2001; Valenzuela et al., 1997). However, in the voltage range of 0 to +70 mV when the inner gate is primarily in the open state, the block was voltage independent (Figure 1d). To probe whether the block by bupivacaine requires repetitive channel openings or has a closed-state dependence, we measured the currents in the absence of bupivacaine ( $I_{\text{ctrl}}$ ) and after 12 min of drug application, whereas the channels were held at  $-80$  mV in the closed state ( $I_{\text{bupi}}$ ) (Figure 1e,f). These recordings revealed that  $K_v1.5$  channels have to be opened before bupivacaine can block the channels and that a rapid open-channel block already reaches steady-state inhibition within the first test pulse (Figure 1e,f).

### 3.2 | Identification of the bupivacaine binding site in the central cavity and side pockets of $K_v1.5$ channels

The binding site of local anaesthetics in the central cavity of  $K_v$  channels has not been systematically mapped using an alanine mutagenesis screen. Strikingly, published data indicate that local anaesthetics might also bind to residues outside the central cavity. Therefore, to characterize the bupivacaine binding site in detail, we performed a functional alanine scanning mutagenesis screen (59 mutants) of the pore-forming S6 segment and the pore signature sequence, together with the S4 segment, the S4–S5 linker and the S5 segment, as these domains form the side pockets of  $K_v1.5$  channels (Figure S4) (Marzian et al., 2013). To this end, the inhibition of bupivacaine for the different  $K_v1.5$  alanine mutants was determined by voltage-clamp recordings in *Xenopus* oocytes. Note that endogenous alanine residues were



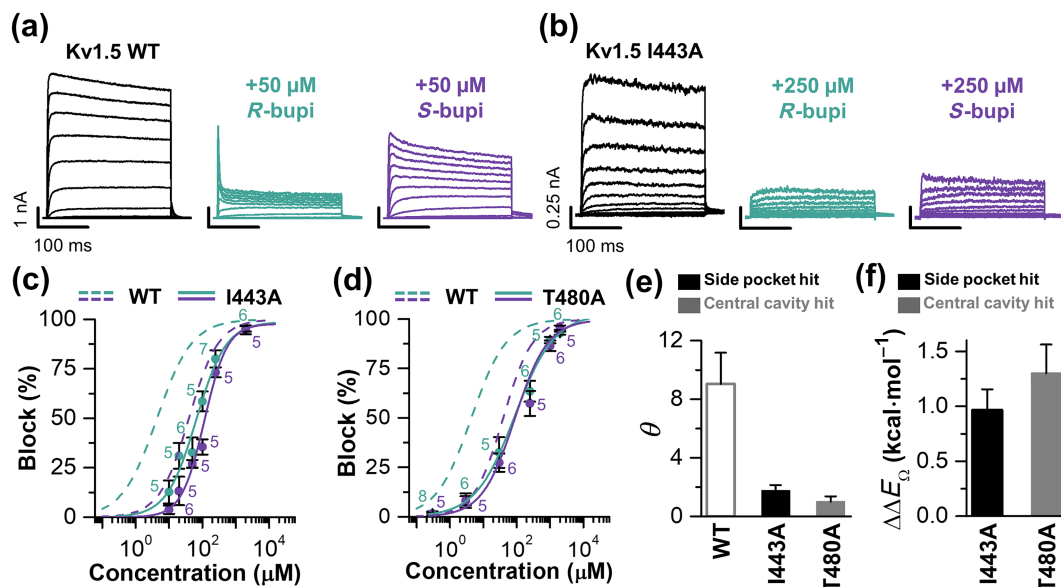
**FIGURE 1** Characterization of the inhibition of  $K_v1.5$  channels by bupivacaine and mapping of the binding site. (a) Representative voltage-clamp recordings of  $K_v1.5$  channels expressed in *Xenopus laevis* oocytes before and after application of 250- $\mu$ M R/S-bupivacaine. (b) Dose-response curve for inhibition of  $K_v1.5$  channels by R/S-bupivacaine. (c)  $G/V$  relationship of  $K_v1.5$  channels in the absence and presence of 250- $\mu$ M R/S-bupivacaine, respectively. (d) Analyses of the voltage dependence of the inhibition of  $K_v1.5$  channels by 250- $\mu$ M R/S-bupivacaine in the voltage range of  $-20$  to  $+70$  mV. (e) Analyses of the use dependence of the inhibition of  $K_v1.5$  channels by R/S-bupivacaine (250  $\mu$ M). The inset illustrates representative  $K_v1.5$  channel currents measured before and the first two pulses directly after a 12-min pulse-free period, during which the drug was washed in, whereas the cells were held at  $-80$  mV. (f) Ratio of  $I_{\text{drug}}$  to  $I_{\text{control}}$  determined for the first voltage step, derived from (e). (g) Representative voltage-clamp recordings of oocytes expressing wild-type  $K_v1.5$  (WT) or the mutant channels before and after application of 250- $\mu$ M R/S-bupivacaine. (h) Alanine scanning of the S4 segment, the S4–S5 linker, and the S5 and S6 segments. Analyses of the inhibition by 250- $\mu$ M R/S-bupivacaine for the mutants and the respective wild-type channels. The values illustrated for the inhibition of S4 segment and S4–S5 linker mutants (dashed bars and box) were previously reported by Marzian et al., 2013. \* $P < .05$ , significantly different from WT. (i) Lack of correlation between the inactivation properties of the identified ‘hit’ mutants and their apparent sensitivity to bupivacaine. The inactivation properties of the mutants were analysed as percentage of inactivation over a time course of 1 s at  $+40$  mV and were derived from the study by Marzian et al. (2013)

mutated to valine. Under these experimental conditions, 250- $\mu$ M bupivacaine caused an  $81.0 \pm 2.0\%$  ( $n = 8$ ) inhibition of wild-type  $K_v1.5$  channels. The working hypothesis of this experimental approach was that a mutant channel lacking its regular amino acid side chain should have a reduced sensitivity to bupivacaine. The potency of bupivacaine was significantly reduced for T480A of the pore signature sequence and I502A, L510A, V512A and V516A of the S6 segment (Figure 1g,h). T480, V512 and V516 are pore-facing amino acids belonging to the classical drug binding site for high-affinity blockers in the central cavity of  $K_v1.5$  channels (Decher et al., 2004, 2006; Marzian et al., 2013; Strutz-Seeböhm et al., 2007), whereas I502 faces into fenestrations connecting the central cavity with the side pockets and L510 directly faces into the side pockets (Marzian et al., 2013). Moreover, we found that three residues (T479, T507 and V514) previously proposed to contribute to the local anaesthetic binding site (Caballero et al., 2002; Franqueza et al., 1997) did not significantly alter bupivacaine inhibition. In contrast, T480 of the pore signature sequence plays a much more pronounced role for the inhibition by the local anaesthetic than the initially proposed T479 (Caballero et al., 2002; Franqueza et al., 1997). Thus, the alanine scan of the S6

segment already revealed revisited and also unexpected results for the binding site of the local anaesthetic bupivacaine (Figure S5).

Most importantly, these results support the idea that bupivacaine interacts with the classical binding site in the central cavity and the selectivity filter as well as with parts of the side pockets of the  $K_v1.5$  channel. Although we reported that mutations in the S4 and S4–S5 linker do not affect inhibition by bupivacaine (Figure 1h, dashed bars and box described by Marzian et al., 2013), the alanine scan of the S5 domain revealed significantly reduced bupivacaine potency for four mutant channels (Figure 1h). The four residues that we identified in S5, L436, F439, F440 and I443 directly face into the side pockets, as does L510 of the S6 segment. These data further support that bupivacaine binds to the central cavity and the side pockets of  $K_v1.5$  channels.

As it was previously proposed that local anaesthetics can bind to the inactivated state of sodium channels, we tested for a correlation between inhibition and the intrinsic inactivation properties of the mutants. However, plotting the extent of C-type inactivation of single mutants against the respective inhibition did not reveal such a correlation (Figures 1i and S6). Furthermore, these mutations seem not to have introduced important modifications in the function of the



**FIGURE 2** Stereoselectivity of the inhibition of  $K_v1.5$  channels by bupivacaine is determined by residues in the central cavity and the side pockets. (a) Whole-cell patch-clamp recordings of wild-type  $K_v1.5$  channels recorded in HEK-293 cells, before and after the application of 50- $\mu$ M R-bupivacaine or S-bupivacaine, respectively. (b) Patch-clamp recordings of I443A, before and after the application of 250- $\mu$ M R-bupivacaine or S-bupivacaine, respectively. (c–e) Dose–response curves of the inhibition of  $K_v1.5$  channels by R-bupivacaine and S-bupivacaine for the (c) I443A and (d) T480A mutants. Dashed lines indicate the respective dose–response curves for inhibition of wild-type  $K_v1.5$  channels by R-bupivacaine and S-bupivacaine described by Arias et al. (2007). (e) Degree of the stereoselectivity ( $\theta$  value) for wild-type  $K_v1.5$  and the I443A and T480A mutant channels. (f) Coupling energies ' $\Delta\Delta E_\Omega$ ' were calculated utilizing a mutant cycle analysis for the I443A and T480A mutants (see Section 2.3 and Figure S1 for further details)

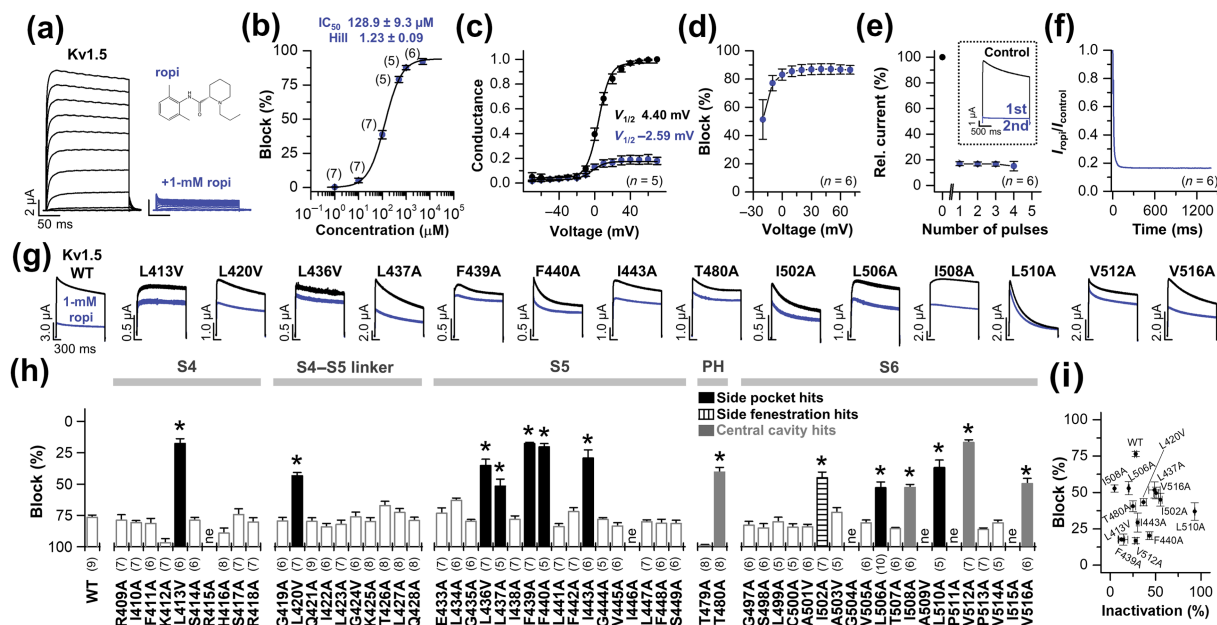
channel, and the differences in the inactivation kinetics are likely due to the variability of slow inactivation of these mutant channels. The extent of C-type inactivation of the mutants is also plotted in Figures 1i, 3i and S6. Thus, the residues identified by our alanine scan most likely exhibit a reduced sensitivity due to an impaired drug binding and not by altered inactivation properties of the mutants.

### 3.3 | Binding to both the central cavity and the side pockets is an important prerequisite for stereoselective inhibition of $K_v1.5$ channels by bupivacaine

Bupivacaine causes a strong stereoselective inhibition of  $K_v1.5$  channels (Arias et al., 2007; Franqueza et al., 1997; Valenzuela, Delpon, et al., 1995) with the R-enantiomer being ninefold ( $\theta$ ) more potent (Figure 2a,e). Mutants at T507, L510 and V514 were previously reported to modulate the stereoselectivity of bupivacaine inhibition (Franqueza et al., 1997). From the  $K_v1.2$  crystal structure, we know by now that these residues are located at the back surface of S6 and face into the side pockets. Strikingly, we found that the S5 mutant I443A caused an almost complete loss of stereoselective inhibition of  $K_v1.5$  channels (Figure 2a,b,c,e).

Mutants at T479 located in the pore signature sequence facing the central cavity did not affect the stereoselectivity of bupivacaine inhibition (Franqueza et al., 1997). In addition, we found that T479A

does not cause a major reduction in bupivacaine inhibition (Figure 1g, h), presumably as the threonine side chain is not perfectly facing into the central cavity. In contrast, mutating the neighbouring residue T480 caused a drastic reduction in affinity to bupivacaine (Figure 1g, h), and an almost complete loss of stereoselective inhibition of  $K_v1.5$  channels by bupivacaine, similar to that observed for the I443A mutant (Figure 2a,d,e). Next, we performed a mutation cycle analyses, taking the R-bupivacaine as the wild-type ligand and the S-bupivacaine as the mutant ligand (Figure S1). The  $\Omega$  values obtained for I443A and T480A were 5.17 and 9.12, respectively. Lack of coupling would yield  $\Omega = 1$ , whereas  $\Omega \neq 1$  would indicate an interaction of some sort, although not necessarily a close physical interaction. To solve this problem, we converted the  $\Omega$  to a coupling energy by  $\Delta\Delta E_\Omega$  (Hidalgo & MacKinnon, 1995) and obtained a value of 0.97 kcal·mol<sup>-1</sup> for I443A and 1.30 kcal·mol<sup>-1</sup> for T480A, respectively (Figure 2f). Coupling energies of around 1 kcal·mol<sup>-1</sup> or more indicate a close physical interaction between a ligand and a residue (Hidalgo & MacKinnon, 1995; Rahman & Luetje, 2017; Schreiber & Fersht, 1995). Therefore, the data and analyses suggest that I443 and T480 are important residues determining the stereoselectivity of the inhibition of  $K_v1.5$  channels by bupivacaine. These experiments show that both residues in the central cavity and in the side pockets are crucial determinants for the stereoselective inhibition of  $K_v1.5$  channels by bupivacaine. The fact that residues in the side pockets determine bupivacaine affinity and stereoselectivity strongly argues for a binding of this local anaesthetic to the side pockets of  $K_v1.5$  channels.



**FIGURE 3** Characterization of the inhibition of  $K_v1.5$  channels by ropivacaine and mapping of the binding site. (a) Representative voltage-clamp recordings of  $K_v1.5$  channels expressed in *Xenopus laevis* oocytes before and after application of 1 mM ropivacaine (ropi). (b) Dose–response curve for inhibition of  $K_v1.5$  channels by ropivacaine. (c)  $G/V$  relationship of  $K_v1.5$  channels in the absence and presence of 1 mM ropivacaine, respectively. (d) Analyses of the voltage dependence of the inhibition of  $K_v1.5$  channels by 1 mM ropivacaine in the voltage range of  $-20$  to  $+70$  mV. (e) Analyses of the use dependence of the inhibition of  $K_v1.5$  channels by 1 mM ropivacaine. The inset illustrates representative  $K_v1.5$  channel currents measured before and the first two pulses directly after a 12-min pulse-free period, during which the drug was washed in, whereas the cells were held at  $-80$  mV. (f) Ratio of  $I_{drug}$  to  $I_{control}$  determined for the first voltage step, derived from (e). (g) Representative voltage-clamp recordings of oocytes expressing wild-type  $K_v1.5$  channels (WT) or the mutant channels before and after application of 1 mM ropivacaine.  $*P < .05$ , significantly different from WT. (h) Alanine scanning of the S4 segment, the S4–S5 linker, and the S5 and S6 segments. Analyses of the inhibition by 1 mM ropivacaine for the mutants and the respective wild-type channels. (i) Lack of correlation between the inactivation properties of the identified ‘hit’ mutants and their apparent sensitivity to ropivacaine. The inactivation properties of the mutants were analysed as percentage of inactivation over a time course of 1 s at  $+40$  mV and were derived from the study by Marzian et al. (2013)

### 3.4 | Identification of the ropivacaine binding site in the central cavity and side pockets of $K_v1.5$ channels

Next, we probed the binding site of ropivacaine (which is the S-enantiomer) that also blocks  $K_v1.5$  channels (Valenzuela et al., 1997), albeit with a reduced stereoselectivity of inhibition ( $\theta = 2.5$ -fold) (Longobardo et al., 1998). The following experiments were performed to probe whether the differential binding sites for these two local anaesthetics actually determine the reduced stereoselectivity and affinity of ropivacaine compared with bupivacaine. First, ropivacaine had an  $IC_{50}$  of  $128.9 \pm 9.3 \mu M$  with a Hill coefficient of  $1.23 \pm 0.09$  (Figure 3a,b and Table S1) and thus was, as previously reported, less potent than bupivacaine. Ropivacaine caused a voltage-independent inhibition in the depolarized voltage range of 0 to  $+70$  mV, without a major shift in the voltage dependence of the activation curve of  $K_v1.5$  channels (Figure 3c,d). Ropivacaine blocked  $K_v1.5$  channels with an open-state affinity (Figure 3e,f), and inhibition was reversible after washout (Figure S3), as observed for bupivacaine.

The potency of ropivacaine was reduced against the S6 segment mutants T480A, L510A, V512A and V516A that face either the pore or the side pockets, as found for bupivacaine (Figure 3h vs. Figure 1h).

For the I502A mutant that faces into fenestrations that connect the central cavity with the side pockets, the effects were somewhat more pronounced, and with L506A and I508A, we identified two additional pore-facing residues to be relevant for the inhibition by ropivacaine. Thus, also for ropivacaine, the results support the idea that the drug interacts with the classical binding site in the central cavity and the selectivity filter, as well as with parts of the side pockets of  $K_v1.5$  channels.

Strikingly, we also identified for ropivacaine L436, F439, F440 and I443 in the S5 segment, residues that face into the side pockets (Figure 3g,h). However, we identified one additional residue in the S5 segment, L437, that faces into fenestrations connecting the side pockets to the central cavity, as I502 does (Marzian et al., 2013). Most importantly, ropivacaine requires interactions with residues of the S4 segment (L413) and the S4–S5 linker (L420), residues that were previously reported to interact with Psora-4 bound to the side pockets (Marzian et al., 2013). Thus, ropivacaine binds to the central cavity and the side pockets of  $K_v1.5$  channels. In addition, ropivacaine, which has a reduced stereoselectivity and affinity, must utilize a different binding site or mode in the side pockets.

Also for ropivacaine, plotting the extent of C-type inactivation of single mutants against their respective inhibition did not reveal a



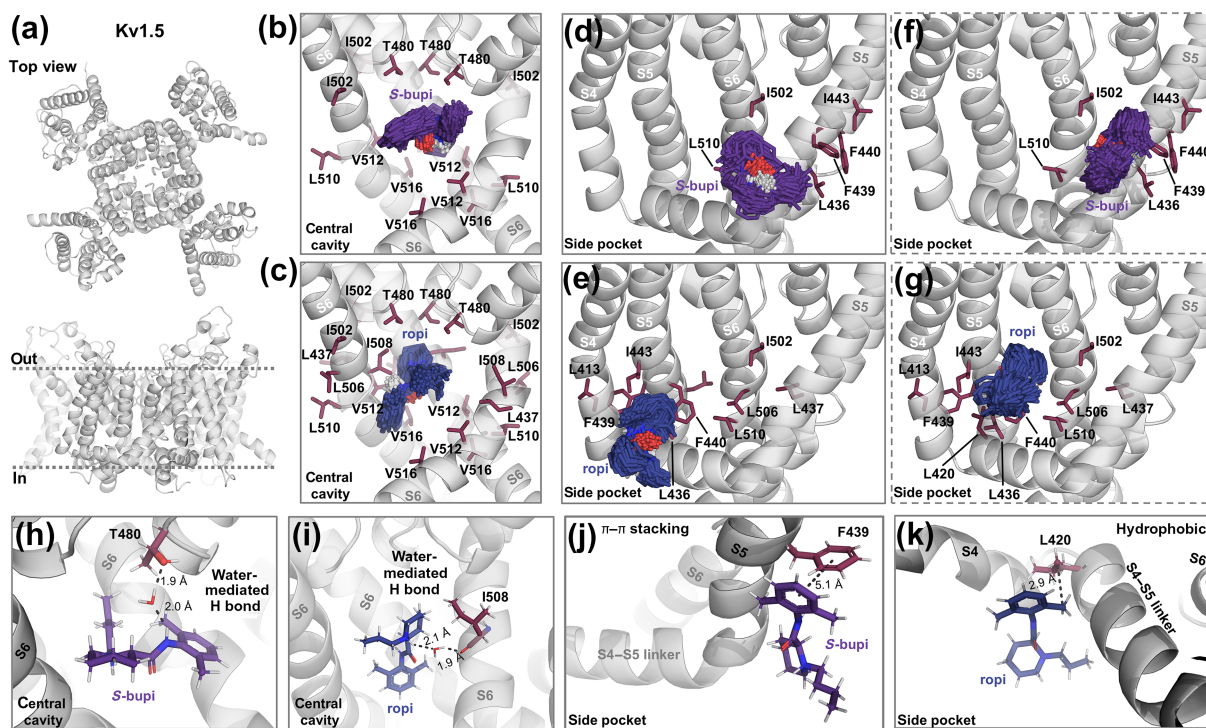
correlation between the inactivation properties of the mutants and their ropivacaine sensitivity (Figures 3i and S6). Thus, the residues identified by our alanine scan most likely exhibit a reduced sensitivity due to an impaired drug binding and not by altered inactivation properties of the mutants.

### 3.5 | Model of the bupivacaine and ropivacaine binding mode in the central cavity and the side pockets of $K_v1.5$ channels

To provide a model for the putative binding sites that we have identified and propose a possible binding mode of bupivacaine, we used *in silico* docking experiments and MD simulations of charged S-bupivacaine and ropivacaine, respectively, using a  $K_v1.5$  homology model based on the r $K_v1.2$ - $K_v2.1$  chimera crystal structure (Figure 4). First, we performed molecular docking experiments to identify the best docking solutions for the central cavity or a single side pocket binding site, separately. Subsequently, we placed the best docking solutions of the side pocket into all four side pockets, leading to an MD starting structure that has a tetrameric and symmetrical structure with four local anaesthetics bound to the side pockets and one to the central cavity. RMSD analysis of the side pockets after 100-ns MDs confirmed that there were no major asymmetries arising in the four

side pockets (Figure S7). Further, we performed 100-ns MD simulations and selected 200 complexes for each binding site (a pose every 0.1 ns from the last 20 ns) to perform a clustering analysis. According to this analysis, we identified highly populated clusters in the central cavity and the side pockets, for both local anaesthetics (Figures 4 and S8). This indicates that in general, both local anaesthetics adopt a fairly stable conformation during the simulation in the central cavity and in the side pockets, because the population of the clusters provides a measure for the stability of the 'drug-to-receptor' interaction. The most populated clusters contained in all cases more than 50% of the total number of 200 conformers. For both local anaesthetics, some clusters were even formed by all or almost all ligand conformers (central cavity and in some of the side pockets; see Figure S8b). Additionally, we have analysed the number of the elements in the most occupied clusters per side pocket and found no significant differences for the conformers between the four different side pockets (Figure S8c). Furthermore, almost half of the ligand surface area was always in contact with the protein during simulations, confirming the reliability of the data (Figure S9).

The proposed binding mode of bupivacaine in the central cavity is illustrated in Figure 4b, illustrating a cluster containing 198 out of 200 conformers. The ropivacaine binding mode is illustrated in Figure 4c, containing 200 out of the 200 conformers. Both local anaesthetics interact with  $K_v1.5$  channels in a somewhat similar mode



**FIGURE 4** Binding modes of S-bupivacaine and ropivacaine in a  $K_v1.5$  channel homology model based on the  $K_v1.2$ - $K_v2.1$  chimera crystal structure (PDB code: 2R9R). Illustration of the binding mode of (b) S-bupivacaine (S-bupi) and (c) ropivacaine (ropi) in the central cavity of the  $K_v1.5$  channel. The most populated clusters are shown, as determined by 100-ns molecular dynamics simulations. Illustration of the most populated cluster or binding mode in the side pockets for (d) S-bupivacaine and for (e) ropivacaine. Illustration of the second most populated cluster or binding mode in the side pockets for (f) S-bupivacaine and for (g) ropivacaine. Illustration of concrete interactions of the two local anaesthetics in (h, i) the central cavity and (j, k) the side pockets



(Figure 4b,c). Although both ligands are predicted to bind with different orientations (Figure S10a,b), the compounds adopt a similar conformation and a similar geometrical positioning of residues that interact with the drugs (indicated by dotted lines), and the nature of interactions is also similar (Figure S10c,d). For both compounds, the most populated cluster (Figure 4b,c) provided the basis for interactions with the residues identified in the alanine mutagenesis scan of the S6 segment (Figures 1h and 3h), except for L510 as this residue is facing into the side pockets.

Figure 4d,f illustrates the two most likely binding modes of bupivacaine in the side pockets of the  $K_v1.5$  channel, representing the two most occupied clusters (containing 200 and 199 conformers). The two most occupied side pockets clusters (containing 200 and 192 conformers) derived from the MD simulations with ropivacaine are illustrated underneath (Figure 4e,g). Note that the two most occupied clusters of bupivacaine are located at the opposite end of the side pockets (Figure 4d,f) compared with ropivacaine (Figure 4e,g). Consistent with our alanine-scanning mutagenesis, ropivacaine interacts with the S4 segment, residues of the proximal S4–S5 linker and the back surface of the S5 and S6 segments of a neighbouring subunit (Figure 4e,g). In contrast, bupivacaine does not bind next to the S4 segment and is interacting with residues of the S5 segment of the same subunit (Figure 4d,f), supporting our initial alanine mutagenesis screen of the S4 and S4–S5 linker in which we did not observe any effects on bupivacaine inhibition (Marzian et al., 2013) (Figure 1h).

Detailed analysis of the nature of interactions revealed that bupivacaine is engaged in water-mediated H bonds with T480 of the pore signature sequence, which we less frequently observed for ropivacaine (Figures 4h and S11). Water-mediated H bonds are less strong than direct H bonds, and the probability of the H bonds that we have observed is low, and the residence time is very short; thus, the primary interactions between the ligand and the protein are hydrophobic in nature. Therefore, it remains unclear whether the water-mediated H bonds with T480 of the pore loop might contribute to the higher potency of bupivacaine compared with ropivacaine. In addition, we observed water-mediated H bonds of both bupivacaine and ropivacaine with the residue I508 (Figures 4i and S11). In the side pockets, we have observed prominent  $\pi$ – $\pi$  interactions of bupivacaine with F439 located at the back surface of the S5 segment (Figure 4j), whereas we found hydrophobic interactions of ropivacaine with the L420 residue of the S4–S5 linker (Figure 4k). A list of specific interactions observed in the MD simulations for the two compounds in the side pockets and the central cavity is provided in Tables S2 and S3.

The lipid solubility is primarily responsible for the potency of local anaesthetics, as it determines the membrane permeability. However, also the inhibitory potency of the drugs might be raised by the formation of more stable drug/channel interactions (Longobardo et al., 1998; Punke & Friederich, 2008), especially in hydrophobic cavities, such as the side pockets described here, as binding sites. In fact, the hydrophobic effect is a major driving force for chemical interactions in aqueous solution between local anaesthetics and proteins. Strikingly, we observed that most of the ‘relevant’ residues identified are hydrophobic (and large). Because ropivacaine has a lower lipid

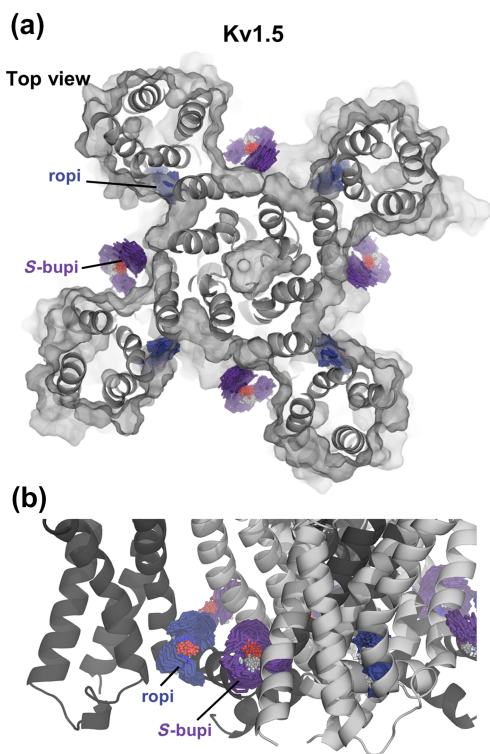
solubility than bupivacaine, we have analysed the hydrophobicity of the different binding sites in the side pockets and found that the binding site of ropivacaine near S4 and the S4–S5 linker is significantly less hydrophobic (Figure S12), which could in part explain the different binding modes of the blockers with highly similar chemical structure.

In our *in silico* experiments, we focused on the *S*-enantiomer of bupivacaine in order to have the best comparison with ropivacaine, which is actually used as a non-racemic drug, the *S*-enantiomer. Using the same stereochemistry for the two compounds in our modelling experiments, the two drugs differ only by the methylene group (propyl vs. butyl side chain). However, as the *R*-conformer is about ninefold more potent, we also performed simulations with *R*-bupivacaine (Figure S13). These findings confirm that the binding sites of bupivacaine and ropivacaine are different within the side pockets, with *R*-bupivacaine also binding more closely to the S5 segment of the same subunit than the S4 segment, similar to *S*-bupivacaine. As expected, we find some differences in the binding mode of the *R*-enantiomer in comparison with *S*-bupivacaine. However, we generally find intrinsic variations for different MD simulations and clusters for any given drug we examine (variance of the system). Thus, we think that it would be too speculative to propose a differential enantioselective binding mode in the side pockets. Thus, for the rest of this study, we kept the experimental design of comparing the two drugs with the same stereochemistry.

Noteworthy, the binding mode of the local anaesthetics and the protein stability of the side pockets appears to be independent of how many side pockets are occupied (Figures S7, S14 and S15), pointing towards a lack of cooperative interactions between the different sites. Taken together, both local anaesthetics bind to the central cavity and the side pockets, albeit binding to the side pockets can occur in two different regions (Figure 5), which might be involved in the fine tuning of stereoselectivity and sensitivity of  $K_v1.x$  channel inhibition by local anaesthetics.

## 4 | DISCUSSION

We propose that local anaesthetics bind to both the central cavity and the side pockets, as a general principle, although there might be differences in the final binding mode of local anaesthetics in the side pockets. Nevertheless, the local anaesthetics bound to the newly identified sites in the side pockets appear to be critical determinants of the potency of the drugs, as mutations in the side pockets strongly diminish the affinity of both compounds bupivacaine and ropivacaine. Besides affecting the apparent affinity, the side pockets contribute to the enantioselectivity shown by bupivacaine for the inhibition of  $K_v1.5$  channels. How these drugs bound in the side pockets ultimately contribute to the efficiency and stereoselectivity of local anaesthetics remains an open question. Given that they cannot cause a pore occlusion from the side pockets, we can only speculate at this time that they exert an allosteric effect on the pore that contributes to channel inhibition. The Hill coefficient near 1 together with the MD simulations that did not provide any evidence towards that drug binding to



**FIGURE 5** Differential binding mode of bupivacaine and ropivacaine in the side pockets of the  $K_v1.5$  channel. (a) Top view of a  $K_v1.5$  homology model based on the  $K_v1.2$ – $K_v2.1$  chimera crystal structure (PDB code: 2R9R) with *S*-bupivacaine (*S*-bupi) and ropivacaine (ropi) bound to the four different side pockets. (b) Side view illustrating the differential binding modes of bupivacaine and ropivacaine. Neighbouring subunits can be distinguished as they are illustrated in grey rather than dark grey

one side pocket has an influence on the protein stability or drug binding at another side pocket, suggests that there is a lack of cooperativity, at least for the local anaesthetic binding to the side pockets. Yet, as we do not know the dissociation constants of all five binding sites, including that in the central cavity, it remains possible that there is some form of cooperativity for the binding of local anaesthetics to the multiple binding sites in  $K_v1.5$  channels. Nevertheless, for an efficient drug block or in the case of bupivacaine for a stereoselective inhibition, binding to both sites, the central cavity and the side pockets, appears to be critical. How many of the four side pockets need to be occupied by local anaesthetic for an efficient channel inhibition remains to be determined. This question is hard to address experimentally, especially as we found that designing concatemeric channels often results in altered biophysical and pharmacological properties.

$K_v1.5$  open-channel blockers exhibit a range of voltage and use dependencies or cooperativity of inhibition. Tikhonov and Zhorov (2014) hypothesized that this might be caused by a common mechanism, meaning that the compounds form a blocking particle itself either by a charged moiety of the drug or by binding of neutral drugs to a potassium ion at the  $S_5$  site in the cavity, using different stoichiometries for the formation of the respective blocking particle

complex. From this common position underneath the selectivity filter ( $S_5$  site), hydrophobic parts of the drugs were proposed either to remain in the central cavity or to laterally protrude into the side fenestrations to interact with I502, a residue relevant for many blockers of  $K_v1.5$  channels. However, we now have found that not only Psora-4 but also ropivacaine and bupivacaine bind to the side pockets to reach I502 from the other side of the fenestrations. Considering the current study, several drugs were now reported to utilize the side pockets to alter drug affinity or, as in the case of bupivacaine, also stereoselectivity. Therefore, the discussed variabilities in the kinetics or cooperativity of  $K_v1.x$  channel inhibition might not be exclusively caused by the formation of different charged drug potassium complexes in the central cavity but also or even exclusively by an additional drug binding in the side pockets.

An open question in the field is how local anaesthetics cause a stereoselective inhibition of  $K_v1.5$  channels. The  $K_v\beta1.3$  subunit, which binds to the central cavity of  $K_v1.5$  channels (Decher et al., 2008), reduces stereoselectivity of bupivacaine inhibition (Arias et al., 2007). Strikingly, the  $\theta$  value is only reduced from about 9 to 4 (Arias et al., 2007), although  $K_v\beta1.3$  interacts with all the directly pore-facing residues that we have also identified as binding sites for local anaesthetics, including T480, I508, V512 and V516 (Decher et al., 2005). These data indicate that there are other residues outside the central cavity that co-determine the stereoselectivity of  $K_v1.5$  channel inhibition by local anaesthetics. Consistent with these data, our mutagenesis data with T480A and I443A indicate that stereoselective inhibition of  $K_v1.5$  channels by bupivacaine is determined by residues in the pore and the side pockets, also further supporting that efficient inhibition by local anaesthetics actually requires binding to both distinct binding sites. For local anaesthetics, it has been shown that reducing the length of the alkyl side chain at the piperidine ring reduces affinity and stereoselectivity (Longobardo et al., 1998). Strikingly, ropivacaine, which has a propyl instead of a butyl side chain compared with bupivacaine and is exhibiting a reduced affinity and almost no stereoselectivity for inhibition of  $K_v1.5$  channels (Longobardo et al., 1998), actually maps to a different binding site in the side pockets, from that for bupivacaine. The ropivacaine binding site determined by *in silico* docking experiments and MD simulations involves interactions with the S4 segment and the proximal S4–S5 linker and a binding to the S5 segment of a neighbouring channel subunit. At the ropivacaine binding site, the interactions with the S5 segment residue I443, which is involved in determining the stereoselective inhibition of bupivacaine, can easily be accomplished, and thus, these residues are presumably accessible for both enantiomers. In contrast, bupivacaine maps to the other site of the side pockets from where it appears that an interaction with the S5 residue I443 from the same subunit might be more restricted and only possible or preferred for one of the enantiomers. The differential set of residues that we have mapped for the two local anaesthetics in the side pockets provides the basis for future studies to carefully elaborate how binding to the side pockets contributes to stereoselective channel inhibition of local anaesthetics. Unfortunately, this hypothesis currently remains untested as *in silico* docking experiments and MD

simulations are methodologically not powerful enough to resolve how this relative small stereoselectivity is achieved for a blocker that also displays a rather low potency of channel inhibition.

Calculating a  $K_D$  by determining the respective on and off rates of a drug provides a more precise estimate of a channel/drug interaction than only recording the percentage of inhibition that can be measured for a mutant. However, such an approach was not feasible for the large-scale alanine scanning studies we performed, testing the inhibition potency of two drugs on 59 mutants. To be able to perform such a large scan, we decided to use the *Xenopus* oocyte expression system that enables a higher throughput. Here, due to the yolk of the oocytes, acting as a lipophilic sink, it is not possible to accurately determine an off rate. Even in the case of a rapid and fully reversible inhibition, the rate limiting step will reflect the redistribution of the drug out of the lipophilic reservoir. For the purpose of our study, which was to map residues that are relevant for the inhibition of  $K_v1.5$  channels by local anaesthetics, recording of an apparent affinity by measuring the reduction in inhibition is to our opinion a suitable approach, also chosen in many previous publications (Marzian et al., 2013; Mitcheson et al., 2000; Rinné et al., 2019). Of course with this approach, we can only identify residues that are relevant for a proper inhibition of the channel, whether this in turn reflects reduced binding or reduced efficiency to induce inhibition or allosteric effects needs to be interpreted with caution. A direct ligand binding assay on the other hand has a major limitation because the simple or pure binding to a protein does not necessarily mean that it is subsequently relevant for the inhibition. Thus, recording the relevance of a mutant by functional studies seems more appropriate if you intend to identify relevant residues for the channel inhibition. Mutations in the side pockets might on the other hand reduce drug affinity by allosteric effects. However, when the side pocket mutations primarily act allosterically, one would expect to identify the same residues independent of the drug tested. The residues identified in the side pockets to be relevant for the inhibition by bupivacaine and ropivacaine differ from each other significantly, and the pattern of residues is also different to that of Psora-4 (Marzian et al., 2013). The assumption that local anaesthetics bind to the side pockets is further supported by the findings in our in silico docking experiment and the extensive MD simulations, which support the relevance of the residues that we identified by our alanine scanning mutagenesis approach.

In earlier studies, it was thought that T479 of the pore signature sequence, together with T507, L510 and V514 of the S6 segment, faces the inner pore of  $K_v1.5$  (Yeola et al., 1996), as mutations at these sites altered the pharmacology of the channel. The crystal structures of the bacterial rKv1.2 channel (Long et al., 2005) revealed that T507, L510 and V514 are not pore facing and instead face into side pockets that we have recently described as drug binding site for the  $K_v1.x$  channel blocker Psora-4 (Marzian et al., 2013). Consistent with these results, we have identified, here, in an alanine-scanning approach a novel binding site for local anaesthetics, which is located outside of the central cavity. Unfortunately, most previous studies used only these limited set of mutants to analyse the putative drug binding sites of [quinidine](#) (Yeola et al., 1996), benzocaine

(Caballero et al., 2002), bupivacaine (Caballero et al., 2002; Franqueza et al., 1997), rupatadine (Caballero et al., 1999) or irbesartan (Moreno et al., 2003). Therefore, it is possible that, apart from Psora-4 and local anaesthetics, many more drugs, including the ones mentioned above, are actually utilizing the side pocket to cause or modulate inhibition of  $K_v1.x$  channels.

Our results reveal that local anaesthetics do not exclusively bind to the central cavity and that binding to the side pockets is important for the action of local anaesthetics, providing the molecular basis of modulation of specificity and stereoselectivity, and thus of the spectrum of side effects of local anaesthetics.

## ACKNOWLEDGEMENTS

We thank Oxana Nowak for technical assistance. The study was supported by the Ministerio de Ciencia e Innovación (MICINN, Spain) Grants SAF2016-75021-R and PID2019-104366RB-C21 (to C.V. and T.G.); the European Regional Development Fund (Fondo Europeo de Desarrollo Regional [FEDER]) and the Instituto de Salud Carlos III CIBERCV programme CB/11/00222 (to C.V. and T.G.); the Consejo Superior de Investigaciones Científicas (CSIC) Grants PIE201820E104 and 2019AEP148 (to C.V.); the Fondo Nacional de Desarrollo Científico y Tecnológico (FONDECYT) 1191133 and the Fondo de Equipamiento Científico y Tecnológico (FONDEQUIP) 160063 grants from ANID (to W.G.); and the Deutsche Forschungsgemeinschaft (DFG) Grant DE1482-4/1 to N.D.

## AUTHOR CONTRIBUTIONS

A.K.K., S.S., S.M. and S.R. conducted the electrophysiological experiments in *Xenopus* oocytes, supervised by N.D. A.d.I.C., D.A.P. and A. V-Z. conducted the electrophysiological experiments in HEK-293 cells, supervised by C.V. and T.G. M.B., D.R., J.C.E.M.M. and B.A.A.R. generated the in silico data, supervised by W.G. S.M. and S.R. generated the mutants. A.K.K. and S.M. analysed the electrophysiological data. A.K.K. performed the statistical analyses, generated the figures and contributed to the manuscript writing. N.D., W.G., T.G. and C.V. conceived and designed the experiments. N.D. supervised the whole project and wrote the manuscript.

## CONFLICT OF INTEREST

The authors declare no conflicts of interest.


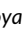





## DECLARATION OF TRANSPARENCY AND SCIENTIFIC RIGOUR

This Declaration acknowledges that this paper adheres to the principles for transparent reporting and scientific rigour of preclinical research as stated in the *BJP* guidelines for [Design & Analysis](#) and [Animal Experimentation](#) and as recommended by funding agencies, publishers and other organizations engaged with supporting research.

## DATA AVAILABILITY STATEMENT

The data supporting the findings of this study are available from the corresponding authors upon reasonable request. Some data may not be made available because of privacy or ethical restrictions.

## ORCID

Aytug K. Kiper  <https://orcid.org/0000-0003-2850-2523>  
 Mauricio Bedoya  <https://orcid.org/0000-0002-3542-7528>  
 David Ramirez  <https://orcid.org/0000-0003-0002-1189>  
 Diego A. Peraza  <https://orcid.org/0000-0002-3913-8619>  
 Susanne Rinné  <https://orcid.org/0000-0003-2326-7069>  
 Carmen Valenzuela  <https://orcid.org/0000-0003-3929-1960>  
 Niels Decher  <https://orcid.org/0000-0002-9433-687X>

## REFERENCES

- Aiyar, J., Nguyen, A. N., Chandy, K. G., & Grissmer, S. (1994). The P-region and S6 of Kv3.1 contribute to the formation of the ion conduction pathway. *Biophysical Journal*, 67(6), 2261–2264. [https://doi.org/10.1016/S0006-3495\(94\)80710-6](https://doi.org/10.1016/S0006-3495(94)80710-6)
- Alexander, S. P. H., Mathie, A., Peters, J. A., Veale, E. L., Striessnig, J., Kelly, E., Armstrong, J. F., Faccenda, E., Harding, S. D., Pawson, A. J., Sharman, J. L., Southan, C., Davies, J. A., & CGTP Collaborators. (2019). The Concise Guide to PHARMACOLOGY 2019/20: Ion channels. *British Journal of Pharmacology*, 176(Suppl 1), S142–S228.
- Arias, C., Guizy, M., David, M., Marzian, S., Gonzalez, T., Decher, N., & Valenzuela, C. (2007). Kv $\beta$ 1.3 reduces the degree of stereoselective bupivacaine block of Kv1.5 channels. *Anesthesiology*, 107(4), 641–651. <https://doi.org/10.1097/01.anes.0000282100.32923.5c>
- Banks, J. L., Beard, H. S., Cao, Y., Cho, A. E., Damm, W., Farid, R., Felts, A. K., Halgren, T. A., Mainz, D. T., Maple, J. R., Murphy, R., Philipp, D. M., Repasky, M. P., Zhang, L. Y., Berne, B. J., Friesner, R. A., Gallicchio, E., & Levy, R. M. (2005). Integrated Modeling Program, Applied Chemical Theory (IMPACT). *Journal of Computational Chemistry*, 26(16), 1752–1780. <https://doi.org/10.1002/jcc.20292>
- Baukrowitz, T., & Yellen, G. (1996). Two functionally distinct subsites for the binding of internal blockers to the pore of voltage-activated K<sup>+</sup> channels. *Proceedings of the National Academy of Sciences*, 93(23), 13357–13361. <https://doi.org/10.1073/pnas.93.23.13357>
- Bennett, P. B., Valenzuela, C., Chen, L. Q., & Kallen, R. G. (1995). On the molecular nature of the lidocaine receptor of cardiac Na<sup>+</sup> channels: Modification of block by alterations in the  $\alpha$ -subunit III-IV interdomain. *Circulation Research*, 77(3), 584–592. <https://doi.org/10.1161/01.RES.77.3.584>
- Bowers, K. J., Chow, D. E., Xu, H., Dror, R. O., Eastwood, M., Gregersen, B. A., Klepeis, J. L., Kolossvary, I., Moraes, M. A., Sacerdoti, F. D., & Salmon, J. K. (2006). Scalable algorithms for molecular dynamics simulations on commodity clusters. ACM/IEEE SC 2006 Conference (SC'06), 43.
- Caballero, R., Moreno, I., Gonzalez, T., Valenzuela, C., Tamargo, J., & Delpon, E. (2002). Putative binding sites for benzocaine on a human cardiac cloned channel (Kv1.5). *Cardiovascular Research*, 56(1), 104–117. [https://doi.org/10.1016/S0008-6363\(02\)00509-6](https://doi.org/10.1016/S0008-6363(02)00509-6)
- Caballero, R., Valenzuela, C., Longobardo, M., Tamargo, J., & Delpon, E. (1999). Effects of rupatadine, a new dual antagonist of histamine and platelet-activating factor receptors, on human cardiac Kv1.5 channels. *British Journal of Pharmacology*, 128(5), 1071–1081. <https://doi.org/10.1038/sj.bjp.0702890>
- Cheng, A., & Merz, K. M. (1996). Application of the Nosé–Hoover chain algorithm to the study of protein dynamics. *The Journal of Physical Chemistry*, 100, 1927–1937. <https://doi.org/10.1021/jp951968y>
- Choi, K. L., Mossman, C., Aube, J., & Yellen, G. (1993). The internal quaternary ammonium receptor site of Shaker potassium channels. *Neuron*, 10(3), 533–541. [https://doi.org/10.1016/0896-6273\(93\)90340-W](https://doi.org/10.1016/0896-6273(93)90340-W)
- Clarkson, C. W., & Hondeghem, L. M. (1985). Mechanism for bupivacaine depression of cardiac conduction: Fast block of sodium channels during the action potential with slow recovery from block during diastole. *Anesthesiology*, 62(4), 396–405. <https://doi.org/10.1097/00000542-198504000-00006>
- Curtis, M. J., Alexander, S., Cirino, G., Docherty, J. R., George, C. H., Giembycz, M. A., Hoyer, D., Insel, P. A., Izzo, A. A., Ji, Y., MacEwan, D. J., Sobey, C. G., Stanford, S. C., Teixeira, M. M., Wonnacott, S., & Ahluwalia, A. (2018). Experimental design and analysis and their reporting II: Updated and simplified guidance for authors and peer reviewers. *British Journal of Pharmacology*, 175(7), 987–993. <https://doi.org/10.1111/bph.14153>
- Decher, N., Gonzalez, T., Streit, A. K., Sachse, F. B., Renigunta, V., Soom, M., Heinemann, S. H., Daut, J., & Sanguinetti, M. C. (2008). Structural determinants of Kv $\beta$ 1.3-induced channel inactivation: A hairpin modulated by PIP<sub>2</sub>. *The EMBO Journal*, 27(23), 3164–3174. <https://doi.org/10.1038/emboj.2008.231>
- Decher, N., Kumar, P., Gonzalez, T., Pirard, B., & Sanguinetti, M. C. (2006). Binding site of a novel Kv1.5 blocker: A “foot in the door” against atrial fibrillation. *Molecular Pharmacology*, 70(4), 1204–1211. <https://doi.org/10.1124/mol.106.026203>
- Decher, N., Kumar, P., Gonzalez, T., Renigunta, V., & Sanguinetti, M. C. (2005). Structural basis for competition between drug binding and Kv $\beta$ 1.3 accessory subunit-induced N-type inactivation of Kv1.5 channels. *Molecular Pharmacology*, 68(4), 995–1005. <https://doi.org/10.1124/mol.105.011668>
- Decher, N., Pirard, B., Bundis, F., Peukert, S., Baringhaus, K. H., Busch, A. E., Steinmeyer, K., & Sanguinetti, M. C. (2004). Molecular basis for Kv1.5 channel block: Conservation of drug binding sites among voltage-gated K<sup>+</sup> channels. *The Journal of Biological Chemistry*, 279(1), 394–400. <https://doi.org/10.1074/jbc.M307411200>
- Fedida, D., Wible, B., Wang, Z., Fermi, B., Faust, F., Nattel, S., & Brown, A. M. (1993). Identity of a novel delayed rectifier current from human heart with a cloned K<sup>+</sup> channel current. *Circulation Research*, 73(1), 210–216. <https://doi.org/10.1161/01.RES.73.1.210>
- Franqueza, L., Longobardo, M., Vicente, J., Delpon, E., Tamkun, M. M., Tamargo, J., Snyders, D. J., & Valenzuela, C. (1997). Molecular determinants of stereoselective bupivacaine block of hKv1.5 channels. *Circulation Research*, 81(6), 1053–1064. <https://doi.org/10.1161/01.RES.81.6.1053>
- Friesner, R. A., Murphy, R. B., Repasky, M. P., Frye, L. L., Greenwood, J. R., Halgren, T. A., Sanschagrin, P. C., & Mainz, D. T. (2006). Extra precision glide: Docking and scoring incorporating a model of hydrophobic enclosure for protein–ligand complexes. *Journal of Medicinal Chemistry*, 49(21), 6177–6196. <https://doi.org/10.1021/jm051256o>
- Gonzalez, T., Longobardo, M., Caballero, R., Delpon, E., Tamargo, J., & Valenzuela, C. (2001). Effects of bupivacaine and a novel local anesthetic, IQB-9302, on human cardiac K<sup>+</sup> channels. *The Journal of Pharmacology and Experimental Therapeutics*, 296(2), 573–583.
- Gonzalez, T., Navarro-Polanco, R., Arias, C., Caballero, R., Moreno, I., Delpon, E., Tamargo, J., Tamkun, M. M., & Valenzuela, C. (2002). Assembly with the Kv $\beta$ 1.3 subunit modulates drug block of hKv1.5 channels. *Molecular Pharmacology*, 62(6), 1456–1463. <https://doi.org/10.1124/mol.62.6.1456>
- Guimaraes, C. R., & Cardozo, M. (2008). MM-GB/SA rescoring of docking poses in structure-based lead optimization. *Journal of Chemical Information and Modeling*, 48(5), 958–970. <https://doi.org/10.1021/ci800004w>
- Halgren, T. (2007). New method for fast and accurate binding-site identification and analysis. *Chemical Biology & Drug Design*, 69(2), 146–148. <https://doi.org/10.1111/j.1747-0285.2007.00483.x>
- Halgren, T. A. (2009). Identifying and characterizing binding sites and assessing druggability. *Journal of Chemical Information and Modeling*, 49(2), 377–389. <https://doi.org/10.1021/ci800324m>
- Hamill, O. P., Marty, A., Neher, E., Sakmann, B., & Sigworth, F. J. (1981). Improved patch-clamp techniques for high-resolution current recording from cells and cell-free membrane patches. *Pflügers Archiv*, 391(2), 85–100. <https://doi.org/10.1007/BF00656997>



- Hanner, M., Green, B., Gao, Y. D., Schmalhofer, W. A., Matyskiela, M., Durand, D. J., Felix, J. P., Linde, A. R., Bordallo, C., Kaczorowski, G. J., Kohler, M., & Garcia, M. L. (2001). Binding of correolide to the  $K_v1.3$  potassium channel: Characterization of the binding domain by site-directed mutagenesis. *Biochemistry*, 40(39), 11687–11697. <https://doi.org/10.1021/bi0111698>
- Hidalgo, P., & MacKinnon, R. (1995). Revealing the architecture of a  $K^+$  channel pore through mutant cycles with a peptide inhibitor. *Science*, 268(5208), 307–310. <https://doi.org/10.1126/science.7716527>
- Hockerman, G. H., Dilmac, N., Scheuer, T., & Catterall, W. A. (2000). Molecular determinants of diltiazem block in domains III<sub>S6</sub> and IV<sub>S6</sub> of L-type  $Ca^{2+}$  channels. *Molecular Pharmacology*, 58(6), 1264–1270. <https://doi.org/10.1124/mol.58.6.1264>
- Humphrey, W., Dalke, A., & Schulten, K. (1996). VMD: Visual molecular dynamics. *Journal of Molecular Graphics*, 14(1), 33–3827-38. [https://doi.org/10.1016/0263-7855\(96\)00018-5](https://doi.org/10.1016/0263-7855(96)00018-5)
- Kaminski, G. A., Friesner, R. A., Tirado-Rives, J., & Jorgensen, W. L. (2001). Evaluation and reparametrization of the OPLS-AA force field for proteins via comparison with accurate quantum chemical calculations on peptides. *The Journal of Physical Chemistry. B*, 105, 6474–6487.
- Kiper, A. K., Rinné, S., Rolfes, C., Ramirez, D., Seebohm, G., Netter, M. F., González, W., & Decher, N. (2015).  $K_v1.5$  blockers preferentially inhibit TASK-1 channels: TASK-1 as a target against atrial fibrillation and obstructive sleep apnea? *Pflügers Archiv—European Journal of Physiology*, 467(5), 1081–1090. <https://doi.org/10.1007/s00424-014-1665-1>
- Kotelko, D. M., Shnider, S. M., Dailey, P. A., Brizgys, R. V., Levinson, G., Shapiro, W. A., Koike, M., & Rosen, M. A. (1984). Bupivacaine-induced cardiac arrhythmias in sheep. *Anesthesiology*, 60(1), 10–18. <https://doi.org/10.1097/0000542-198401000-00004>
- Lilley, E., Stanford, S. C., Kendall, D. E., Alexander, S. P., Cirino, G., Docherty, J. R., George, C. H., Insel, P. A., Izzo, A. A., Ji, Y., Panettieri, R. A., Sobey, C. G., Stefanska, B., Stephens, G., Teixeira, M., & Ahluwalia, A. (2020). ARRIVE 2.0 and the British Journal of Pharmacology: Updated guidance for 2020. *British Journal of Pharmacology*, 117(16), 3611–3616. <https://doi.org/10.1111/bph.15178>
- Lipka, L. J., Jiang, M., & Tseng, G. N. (1998). Differential effects of bupivacaine on cardiac  $K^+$  channels: Role of channel inactivation and subunit composition in drug-channel interaction. *Journal of Cardiovascular Electrophysiology*, 9(7), 727–742. <https://doi.org/10.1111/j.1540-8167.1998.tb00960.x>
- Long, S. B., Campbell, E. B., & MacKinnon, R. (2005). Crystal structure of a mammalian voltage-dependent Shaker family  $K^+$  channel. *Science*, 309(5736), 897–903. <https://doi.org/10.1126/science.1116269>
- Long, S. B., Tao, X., Campbell, E. B., & MacKinnon, R. (2007). Atomic structure of a voltage-dependent  $K^+$  channel in a lipid membrane-like environment. *Nature*, 450(7168), 376–382. <https://doi.org/10.1038/nature06265>
- Longobardo, M., Delpon, E., Caballero, R., Tamargo, J., & Valenzuela, C. (1998). Structural determinants of potency and stereoselective block of hKv1.5 channels induced by local anesthetics. *Molecular Pharmacology*, 54(1), 162–169. <https://doi.org/10.1124/mol.54.1.162>
- Martyna, G. J., Tobias, D. J., & Klein, M. L. (1994). Constant pressure molecular dynamics algorithms. *The Journal of Chemical Physics*, 101, 4177–4189. <https://doi.org/10.1063/1.467468>
- Marzian, S., Stansfeld, P. J., Rapedius, M., Rinné, S., Nematian-Ardestani, E., Abbruzzese, J. L., Steinmeyer, K., Sansom, M. S. P., Sanguinetti, M. C., Baukrowitz, T., & Decher, N. (2013). Side pockets provide the basis for a new mechanism of Kv channel-specific inhibition. *Nature Chemical Biology*, 9(8), 507–513. <https://doi.org/10.1038/nchembio.1271>
- Mitcheson, J. S., Chen, J., Lin, M., Culberson, C., & Sanguinetti, M. C. (2000). A structural basis for drug-induced long QT syndrome. *Proc Natl Acad Sci USA*, 97(22), 12329–12333. <https://doi.org/10.1073/pnas.210244497>
- Moreno, I., Caballero, R., Gonzalez, T., Arias, C., Valenzuela, C., Iriepa, I., Gálvez, E., Tamargo, J., & Delpon, E. (2003). Effects of irbesartan on cloned potassium channels involved in human cardiac repolarization. *The Journal of Pharmacology and Experimental Therapeutics*, 304(2), 862–873. <https://doi.org/10.1124/jpet.102.042325>
- Percie du Sert, N., Hurst, V., Ahluwalia, A., Alam, S., Avey, M. T., Baker, M., Browne, W. J., Clark, A., Cuthill, I. C., Dirnagl, U., Emerson, M., Garner, P., Holgate, S. T., Howells, D. W., Karp, N. A., Lazic, S. E., Lidster, K., MacCallum, C. J., Macleod, M., ... Würbel, H. (2020). The ARRIVE guidelines 2.0: Updated guidelines for reporting animal research. *PLoS Biology*, 18(7), e3000410. <https://doi.org/10.1371/journal.pbio.3000410>
- Punke, M. A., & Friederich, P. (2008). Lipophilic and stereospecific interactions of amino-amide local anesthetics with human  $K_v1.1$  channels. *Anesthesiology*, 109(5), 895–904. <https://doi.org/10.1097/ALN.0b013e31818958c8>
- Rahman, S., & Luetje, C. W. (2017). Mutant cycle analysis identifies a ligand interaction site in an odorant receptor of the malaria vector *Anopheles gambiae*. *The Journal of Biological Chemistry*, 292(46), 18916–18923. <https://doi.org/10.1074/jbc.M117.810374>
- Ramirez, D., Arevalo, B., Martinez, G., Rinné, S., Sepulveda, F. V., Decher, N., & Gonzalez, W. (2017). Side fenestrations provide an “anchor” for a stable binding of A1899 to the pore of TASK-1 potassium channels. *Molecular Pharmacology*, 14(7), 2197–2208. <https://doi.org/10.1021/acs.molpharmaceut.7b00005>
- Rinné, S., Kiper, A. K., Vowinkel, K. S., Ramirez, D., Schewe, M., Bedoya, M., Aser, D., Gensler, I., Netter, M. F., Stansfeld, P. J., Baukrowitz, T., Gonzalez, W., & Decher, N. (2019). The molecular basis for an allosteric inhibition of  $K^+$ -flux gating in  $K_{2P}$  channels. *eLife*, 8, e39476. <https://doi.org/10.7554/eLife.39476>
- Sali, A., & Blundell, T. L. (1993). Comparative protein modelling by satisfaction of spatial restraints. *Journal of Molecular Biology*, 234(3), 779–815. <https://doi.org/10.1006/jmbi.1993.1626>
- Sanchez-Chapula, J. (1988). Effects of bupivacaine on membrane currents of guinea-pig ventricular myocytes. *European Journal of Pharmacology*, 156(3), 303–308. [https://doi.org/10.1016/0014-2999\(88\)90274-9](https://doi.org/10.1016/0014-2999(88)90274-9)
- Schreiber, G., & Fersht, A. R. (1995). Energetics of protein-protein interactions: Analysis of the Barnase-Barstar interface by single mutations and double mutant cycles. *Journal of Molecular Biology*, 248(2), 478–486. [https://doi.org/10.1016/S0022-2836\(95\)80064-6](https://doi.org/10.1016/S0022-2836(95)80064-6)
- Scott, D. B., Lee, A., Fagan, D., Bowler, G. M., Bloomfield, P., & Lundh, R. (1989). Acute toxicity of ropivacaine compared with that of bupivacaine. *Anesthesia and Analgesia*, 69(5), 563–569.
- Shieh, C. C., & Kirsch, G. E. (1994). Mutational analysis of ion conduction and drug binding sites in the inner mouth of voltage-gated  $K^+$  channels. *Biophysical Journal*, 67(6), 2316–2325. [https://doi.org/10.1016/S0006-3495\(94\)80718-0](https://doi.org/10.1016/S0006-3495(94)80718-0)
- Shivakumar, D., Williams, J., Wu, Y., Damm, W., Shelley, J., & Sherman, W. (2010). Prediction of absolute solvation free energies using molecular dynamics free energy perturbation and the OPLS force field. *Journal of Chemical Theory and Computation*, 6(5), 1509–1519. <https://doi.org/10.1021/ct900587b>
- Snyders, D. J., Tamkun, M. M., & Bennett, P. B. (1993). A rapidly activating and slowly inactivating potassium channel cloned from human heart. Functional analysis after stable mammalian cell culture expression. *The Journal of General Physiology*, 101(4), 513–543. <https://doi.org/10.1085/jgp.101.4.513>
- Streit, A. K., Netter, M. F., Kempf, F., Walecki, M., Rinné, S., Bolleballi, M. K., Preisig-Müller, R., Renigunta, V., Daut, J., Baukrowitz, T., Sansom, M. S. P., Stansfeld, P. J., & Decher, N. (2011). A specific two-pore domain potassium channel blocker defines the structure of the TASK-1 open pore. *The Journal of Biological Chemistry*, 286(16), 13977–13984. <https://doi.org/10.1074/jbc.M111.227884>



- Strutz-Seeböhm, N., Gutcher, I., Decher, N., Steinmeyer, K., Lang, F., & Seeböhm, G. (2007). Comparison of potent Kv1.5 potassium channel inhibitors reveals the molecular basis for blocking kinetics and binding mode. *Cellular Physiology and Biochemistry*, 20(6), 791–800. <https://doi.org/10.1159/000110439>
- Stühmer, W. (1992). Electrophysiological recording from *Xenopus* oocytes. *Methods in Enzymology*, 207, 319–339. [https://doi.org/10.1016/0076-6879\(92\)07021-F](https://doi.org/10.1016/0076-6879(92)07021-F)
- Tikhonov, D. B., & Zhorov, B. S. (2014). Homology modeling of Kv1.5 channel block by cationic and electroneutral ligands. *Biochimica et Biophysica Acta*, 1838(3), 978–987. <https://doi.org/10.1016/j.bbamem.2013.11.019>
- Valenzuela, C., Delpon, E., Franqueza, L., Gay, P., Snyders, D. J., & Tamargo, J. (1997). Effects of ropivacaine on a potassium channel (hKv1.5) cloned from human ventricle. *Anesthesiology*, 86(3), 718–728. <https://doi.org/10.1097/00000542-199703000-00025>
- Valenzuela, C., Delpon, E., Tamkun, M. M., Tamargo, J., & Snyders, D. J. (1995). Stereoselective block of a human cardiac potassium channel (Kv1.5) by bupivacaine enantiomers. *Biophysical Journal*, 69(2), 418–427. [https://doi.org/10.1016/S0006-3495\(95\)79914-3](https://doi.org/10.1016/S0006-3495(95)79914-3)
- Valenzuela, C., Snyders, D. J., Bennett, P. B., Tamargo, J., & Hondeghem, L. M. (1995). Stereoselective block of cardiac sodium channels by bupivacaine in guinea pig ventricular myocytes. *Circulation*, 92(10), 3014–3024. <https://doi.org/10.1161/01.CIR.92.10.3014>
- Yellen, G., Jurman, M. E., Abramson, T., & MacKinnon, R. (1991). Mutations affecting internal TEA blockade identify the probable pore-forming region of a K<sup>+</sup> channel. *Science*, 251(4996), 939–942. <https://doi.org/10.1126/science.2000494>
- Yeola, S. W., Rich, T. C., Uebele, V. N., Tamkun, M. M., & Snyders, D. J. (1996). Molecular analysis of a binding site for quinidine in a human cardiac delayed rectifier K<sup>+</sup> channel: Role of S6 in antiarrhythmic drug binding. *Circulation Research*, 78(6), 1105–1114. <https://doi.org/10.1161/01.RES.78.6.1105>

## SUPPORTING INFORMATION

Additional supporting information may be found online in the Supporting Information section at the end of this article.

**How to cite this article:** Kiper AK, Bedoya M, Stalke S, et al. Identification of a critical binding site for local anaesthetics in the side pockets of K<sub>v</sub>1 channels. *Br J Pharmacol*. 2021;178: 3034–3048. <https://doi.org/10.1111/bph.15480>